

A novel Cu(II) chemical vapor deposition precursor: Synthesis, characterization, and chemical vapor deposition

Anjana Devi, J. Goswami, R. Lakshmi, and S. A. Shivashankar
Materials Research Centre, Indian Institute of Science, Bangalore-560 012 India

S. Chandrasekaran
Department of Organic Chemistry, Indian Institute of Science, Bangalore-560 012 India

(Received 13 January 1997; accepted 25 June 1997)

A nonfluorinated β -diketonate precursor, bis(*t*-butylacetoacetato)Cu(II) or Cu(tbaoac)₂, was synthesized by modifying bis(dipivaloylmethanato)Cu(II) or Cu(dpm)₂ for chemical vapor deposition (CVD) of copper. The complex was characterized by a variety of techniques, such as melting point determination, mass spectrometry, infrared spectroscopy, elemental analysis, thermogravimetric and differential thermal analysis, and x-ray diffraction. Cu(tbaoac)₂ has a higher sublimation rate than Cu(dpm)₂ over the temperature range 90–150 °C. Pyrolysis of Cu(tbaoac)₂ leads to the formation of copper films at 225 °C, compared to 330 °C for Cu(dpm)₂. As-deposited copper films were highly dense, mirror-bright, adhered strongly to SiO₂, and showed a resistivity of less than 2.9 $\mu\Omega$ -cm at a thickness as low as 1300 Å. A possible mechanism for the decomposition of the ligand tbaoac has been proposed.

I. INTRODUCTION

Chemical vapor deposition (CVD) is a versatile process for the preparation of thin films of a variety of materials, such as metals, semiconductors, oxide superconductors, and oxide ferroelectrics.^{1–10} Choosing the optimal precursor with high volatility and thermal stability during its evaporation and transport, and with a low reaction temperature, is a considerable challenge. Various organic ligands have been employed to synthesize metal-organic (MO) precursors, for example, the β -diketonate class of complexes like the acetylacetonates(acac), hexafluoroacetylacetonates(hfac), and dipivaloylmethanates(dpm), and alkoxides of different metals. These compounds have been used as precursors for CVD of metals like Cu, superconductors like YBa₂Cu₃O_{7-x}, and other oxides.^{11–15} In particular, a variety of β -diketonate complexes of copper have been investigated in recent years for suitability as precursors for the CVD of copper, a process of great potential importance in the metallization of VLSI circuits.^{15–21} Of these, the acac and dpm complexes have been found to be insufficiently volatile, leading to low deposition rates.²² Fluorinated Cu(I) and Cu(II) β -diketonates (hfac-based) have led both to high rates of deposition and to significantly lower deposition temperatures.^{23–25} However, fluorination makes precursor handling more difficult, which it is very desirable to avoid. Additionally, hfac-based Cu(I) precursors, even when ligand-stabilized, have poor thermal characteristics and short shelf life.²⁶

The goal of the present work was therefore to design and synthesize a new β -diketonate precursor by modifying the dpm ligand, without fluorination, to

increase the sublimation rate and lower the pyrolysis temperature. The ligand *t*-butylacetoacetate(tbaoac) which has a *t*-butyl ester group, β to the carbonyl group was considered for this purpose because the presence of electronegative oxygen may be expected to produce a more repulsive shell around the complex, reducing the strength of metal-oxygen bonding and thereby increasing the volatility. The ligand tbaoac was chelated with Cu to synthesize a new Cu(II) precursor, namely bis(*t*-butylacetoacetato)Cu(II) or Cu(tbaoac)₂. Figure 1 shows the molecular structures of Cu(dpm)₂ and Cu(tbaoac)₂. In this paper, we report the synthesis and characterization of Cu(tbaoac)₂, including a detailed comparative study of thermal properties of Cu(tbaoac)₂ and Cu(dpm)₂. We also report its application to CVD of thin copper films.

II. EXPERIMENTAL

A. Synthesis and characterization of bis(*t*-butylacetoacetato)copper(II):

The ligand *t*-butylacetoacetate (3.16 g, 0.02 moles, Fluka) in ethanol was buffered with potassium acetate (1.96 g, 0.02 moles, AR grade) and stirred in ice-cold conditions. A hot aqueous solution of cupric acetate (2.0 g, 0.01 moles, AR grade) was added dropwise. The mixture was stirred continuously for 3–4 h in ice-cold conditions to yield a green-colored precipitate (yield = 70%). The chelate was filtered, washed with a mixture of water and ethanol, and suction-dried. It was then recrystallized in hexane. Green, thin, platelet-like single crystals of dimensions up to 10 × 10 mm² were obtained by slow evaporation from hexane.

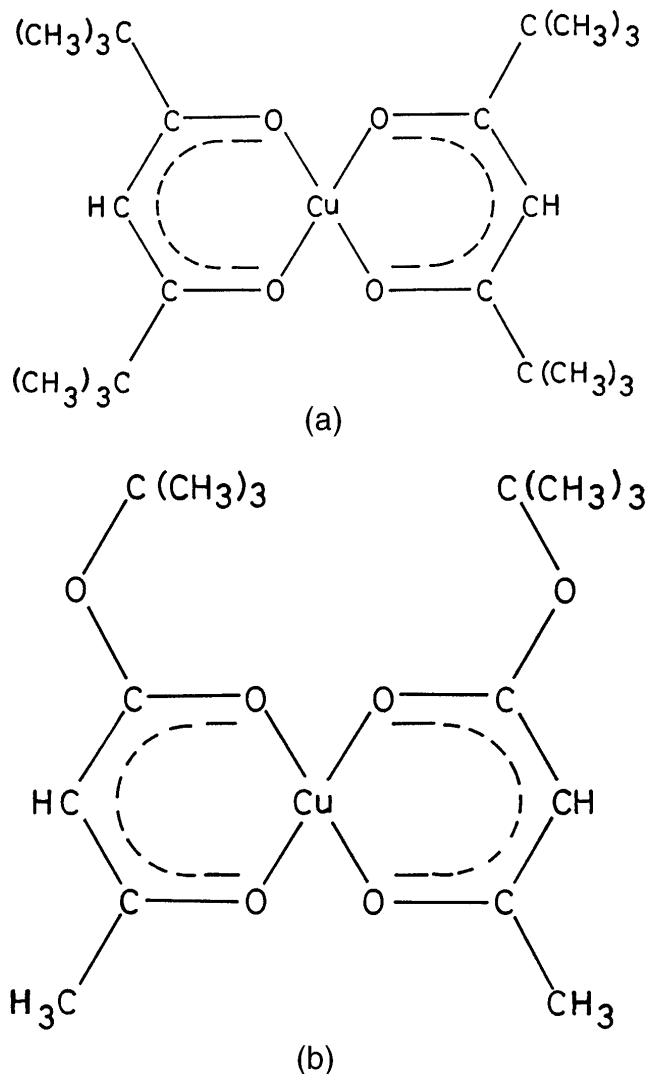


FIG. 1. Molecular structures: (a) $\text{Cu}(\text{dpm})_2$ and (b) $\text{Cu}(\text{tbaoac})_2$.

The copper complex was characterized by a variety of techniques like melting point determination, elemental analysis, mass spectrometry, infrared spectroscopy, thermal analysis (TGA/DTA), and single-crystal x-ray diffraction.

The mass spectrum was recorded on a JEOL JMA-DA5000 mass spectrometer. The IR spectrum of $\text{Cu}(\text{tbaoac})_2$ in KBr matrix (spectroscopic grade) was recorded using an IR spectrometer (Perkin-Elmer 781). The thermal analysis was carried out using the simultaneous TG/DTA analyzer (STA1500, Polymer Laboratories). Single-crystal x-ray diffraction data on $\text{Cu}(\text{tbaoac})_2$ were obtained on a Siemens single crystal diffractometer using $\text{Mo K}\alpha$ ($\lambda = 0.7107 \text{ \AA}$) radiation in $\omega/2\theta$ scan mode up to a maximum 2θ value of 25° .

B. MOCVD

Reduced pressure MOCVD was carried out in a system built in-house, consisting of a cold wall stainless

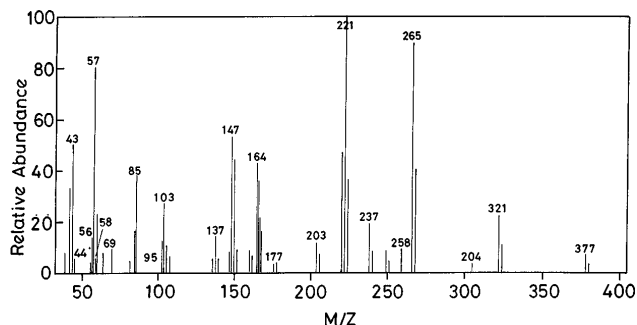
steel reactor with downward vertical flow arrangement.²⁷ Films were deposited on thermally oxidized silicon (100) substrates ($20 \times 20 \text{ mm}^2$). A graphite block was used as substrate support and was heated by quartz halogen lamps. Substrate temperature was controlled through a thermocouple kept inside the graphite block. The accuracy of substrate temperature measurement (to within $\pm 5^\circ \text{C}$) was ensured by conducting dummy growth runs under various conditions on substrates to which a thermocouple was glued using silver paint. The precursor was evaporated from a stainless steel vaporizer maintained at appropriate temperatures. The temperature of the vaporizer, which was kept in an oil bath to ensure uniform heating, was controlled to within $\pm 1^\circ \text{C}$. High purity argon (99.995%) was used as carrier gas. The precursor was fed into the reactor through heated lines to avoid condensation. The reactor was first evacuated below 10^{-4} Torr with a Roots pump of capacity 2500 lit/min. The flow of argon gas was regulated by electronic mass flow controllers. The total pressure of the reactor was measured by a capacitance manometer and was controlled manually during depositions by a throttle valve placed at the inlet of the pump. Manual control of pressure was required only because of the mechanical instability of the bellows-sealed throttle valve. The vapor pressure of the precursor used, as deduced from sublimation rate measurements, is about 0.02 Torr at 100°C . The CVD was conducted at a reactor pressure of 10 Torr. Thus, any increase in reactor pressure due to precursor decomposition would be very small and beyond the sensitivity of the pressure transducer employed.

Films were characterized for their resistivity by the van der Pauw method, surface morphology by scanning electron microscopy (SEM) and optical microscopy, crystallinity by x-ray diffraction, and for composition by x-ray photoelectron spectroscopy (XPS). Average film thickness was calculated by measuring on a semi-microbalance (Mettler 240) the weight gained by the substrate due to deposition (the weight gain due to a film of thickness $\sim 1000 \text{ \AA}$ and measuring 400 mm^2 in area was 0.36 mg).

III. RESULTS AND DISCUSSION

A. Precursor characterization

In the mass spectrum (Fig. 2), the parent peak of $\text{Cu}(\text{tbaoac})_2$, i.e., $(\text{C}_{16}\text{H}_{26}\text{O}_6)\text{Cu}$, $m/z = 377$, corresponds to the molecular weight of the complex and thus confirms the formation of the complex. The other major peaks of the various fragments of the complex are as follows: The base peak at $m/z = 221$ corresponds to $(\text{C}_8\text{H}_{14}\text{O}_3)\text{Cu}$. The peaks at $m/z = 57, 85, 147,$ and 265 correspond to C_4H_9 (*t*-butyl), $\text{C}_5\text{H}_9\text{O}$, $(\text{C}_4\text{H}_4\text{O}_2)\text{Cu}$, and $(\text{C}_8\text{H}_{10}\text{O}_6)\text{Cu}$, respectively. The other fragments at 43, 44, 56, 58, 102, 164, 237, and 321 correspond to

FIG. 2. Mass spectrum of Cu(tbaoac)₂.

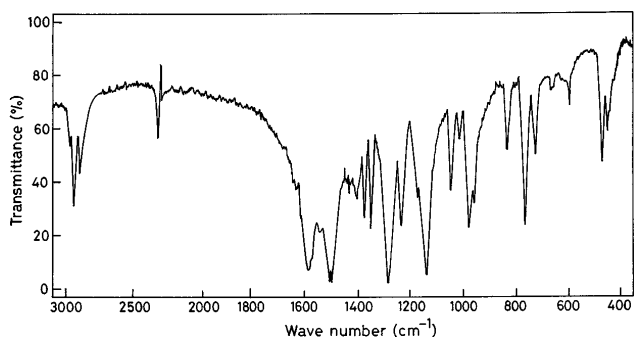
C₂H₃O (acetyl), CO₂ (carbon dioxide), C₄H₈ (isobutene), C₃H₆O (acetone), C₄H₆O₃, (C₄H₅O₃)Cu, (C₇H₁₀O₅)Cu, and (C₁₂H₁₈O₆)Cu, respectively.

The copper complex showed a complicated infrared (IR) spectrum because of the strong mode couplings (Fig. 3). The spectrum showed sharp peaks in the chelate carbonyl region (1400–1630 cm⁻¹), indicating the presence of enolic β-ketoester, while the metal-oxygen peak at 480 cm⁻¹ confirmed the formation of the desired complex. The peaks in the region 2872–2962 cm⁻¹ correspond to CH₃.

Elemental analysis of single crystals of the material gave the following calculated (found) atomic percentages: C, 50.86 (49.99); H, 6.88 (6.69). These data confirm that the desired complex had been obtained.

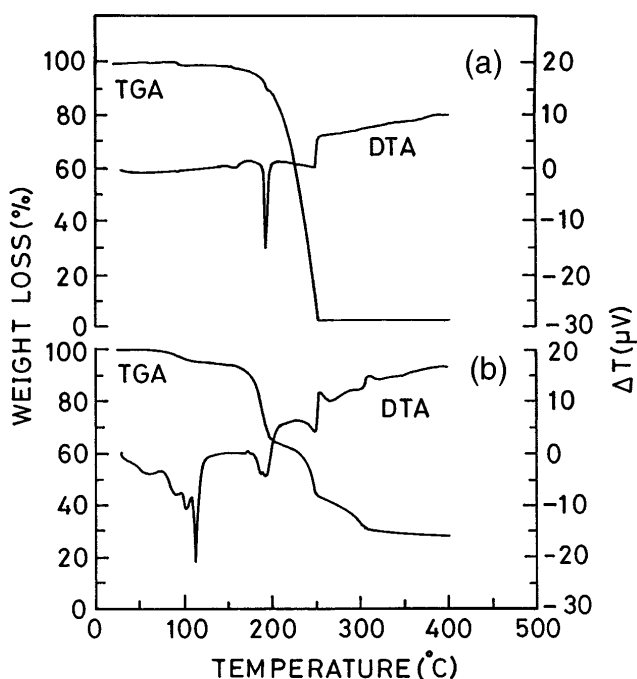
Structure refinement using single crystal XRD data shows that the compound crystallizes in the orthorhombic system, belonging to space group *Pnma* with *a* = 9.558 Å, *b* = 20.676 Å, *c* = 9.591 Å, and *Z* = 4. Details of the crystal structure have been published elsewhere.²⁸

Thermogravimetry (TG) has been used as an effective tool for the rapid determination of the relative volatilities of various metal β-diketonates.²⁹ A detailed thermal analysis of Cu(tbaoac)₂ was therefore carried out to evaluate its suitability as a CVD precursor. This is also required to optimize the temperature at which the precursor vaporizer should be maintained during CVD. Simultaneous thermogravimetric and differential

FIG. 3. Infrared spectrum of Cu(tbaoac)₂.

thermal analysis (TG/DTA) were carried out at atmospheric pressure over the temperature range 25–400 °C with 10 °C/min heating rate, using ~10 mg of finely powdered sample. To mimic the ambient used eventually in the CVD chamber, TG/DTA was done under flowing high purity argon (99.995%, 20 sccm). The comparative TG/DTA of Cu(dpm)₂ and Cu(tbaoac)₂ is as shown in Fig. 4. The melting points of (a) Cu(dpm)₂ and (b) Cu(tbaoac)₂ are 192 °C and 110 °C, respectively, as revealed by the DTA results. These are in full agreement with the melting points of the respective complexes measured in a sealed capillary tube. The TGA data for Cu(dpm)₂ show a monotonic weight loss with temperature, with virtually no residue, whereas the data for Cu(tbaoac)₂ show a complex behavior including a residual of about 22% of the original weight. The latter begins to decompose at a low temperature of about 190 °C, which indicates that deposition of Cu by MOCVD may be possible at a reduced substrate temperature, as desired.

In a CVD process where precursors are solid materials, the sublimation rate of the precursor in the flowing carrier gas ambient actually determines the rate of precursor delivery into the reactor. Using the TG analyzer, a detailed study was conducted to determine the weight loss of the complex as a function of time for different sublimation temperatures. To keep the sample surface area constant, for every experiment, the sample crucible was densely filled by a fine powder of the material of nearly the same initial weight (~17 mg). All the experiments were carried out under flowing argon (40 sccm)

FIG. 4. Simultaneous TGA and DTA: (a) Cu(dpm)₂ and (b) Cu(tbaoac)₂ under flowing Ar (20 sccm).

environment. Figure 5 shows the comparative study of the sublimation of the two precursors (a) $\text{Cu}(\text{dpm})_2$ and (b) $\text{Cu}(\text{tbaaac})_2$ at 120 °C and 95 °C, respectively. The data were recorded after the sample temperature had stabilized. Sublimation rates of $\text{Cu}(\text{dpm})_2$ and $\text{Cu}(\text{tbaaac})_2$ are 2.18×10^{-3} mg/min at 120 °C and 2.37×10^{-3} mg/min at 95 °C, respectively. The constant slopes obtained show that the sublimation rate of the precursors remain unchanged over a length of time similar to that involved in a typical CVD growth run employed in this study. Figure 6 shows sublimation rates of the two precursors at different temperatures, calculated from the slope of the weight loss versus time curves. These data show that, at a given temperature, $\text{Cu}(\text{tbaaac})_2$ has a higher sublimation rate than $\text{Cu}(\text{dpm})_2$. Thus, compared to $\text{Cu}(\text{dpm})_2$, the sublimation of $\text{Cu}(\text{tbaaac})_2$ should result in higher precursor flow rate; i.e., it could be a useful precursor for the CVD of Cu.

B. Film deposition and analysis

Pyrolysis of $\text{Cu}(\text{tbaaac})_2$ results in the deposition of metallic copper at a substrate temperature as low as 225 °C compared to 330 °C, the threshold temperature for the deposition of Cu from $\text{Cu}(\text{dpm})_2$.²⁷ In the reactor as-designed, a growth rate of 2.7 nm/min under the conditions of 285 °C substrate temperature and 10 Torr reactor pressure was obtained for $\text{Cu}(\text{tbaaac})_2$. Growth is thermally activated in the narrow temperature range of 225 to 320 °C, where the activation energy is 45.7 kJ/mol. The as-deposited copper films are very smooth and mirror bright, with a dense microstructure as revealed by the SEM micrograph shown in Fig. 7. The grains are very small, averaging about 30 nm in size. It is remarkable that, although the deposition temperature is as high as 285 °C, the average grain size is so small. In general, as-deposited copper films are polycrystalline

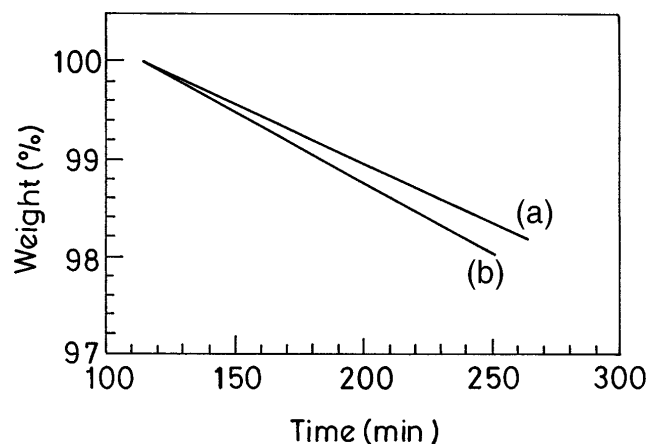


FIG. 5. Weight loss (%) as a function of time: (a) $\text{Cu}(\text{dpm})_2$ and (b) $\text{Cu}(\text{tbaaac})_2$ deduced from TGA data. Amount of starting material = 17 mg.

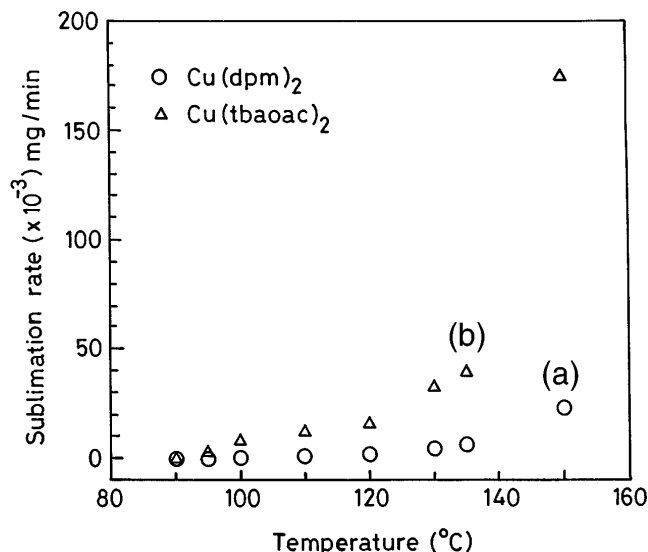


FIG. 6. Sublimation rate as a function of temperature: (a) $\text{Cu}(\text{dpm})_2$ and (b) $\text{Cu}(\text{tbaaac})_2$.

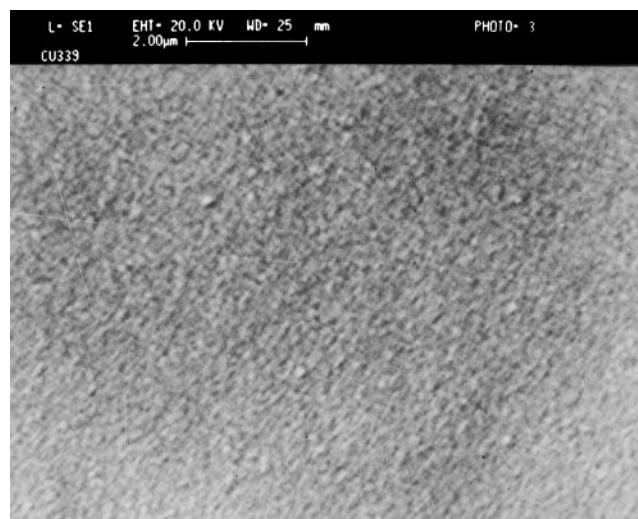


FIG. 7. SEM micrograph of Cu film grown from $\text{Cu}(\text{tbaaac})_2$. Substrate temperature = 225 °C, pressure = 10 Torr, vaporizer temperature = 90 °C, Ar carrier flow = 50 sccm, and film thickness = 30 nm.

with a slight preference for the (111) plane being parallel to the substrate. The intensity ratio of (111) and (200) peaks is 100/16 compared to 100/46 for polycrystalline bulk copper (JCPDS File No. 4-836). The fine-grained structure appears to be the cause of the strong adhesion of the copper film to the SiO_2 substrate surface, as revealed by the scotch tape test. This is in contrast to the poor adhesion of Cu to SiO_2 generally reported, necessitating an adhesion promoter layer between Cu and SiO_2 in the metallization schemes proposed for VLSI.^{17,30-32}

The room-temperature electrical resistivity of as-deposited copper films on SiO_2 has been measured as a

function of film thickness for $\text{Cu}(\text{tbaoc})_2$ (Fig. 8). The film resistivity decreases abruptly to below $4 \mu\Omega\text{-cm}$ at a thickness of $\sim 50 \text{ nm}$ due to the formation of dense and well-connected microstructure at an early stage of growth as observed in SEM micrograph (Fig. 7). This result contrasts with earlier reports where similar connectivity in CVD-grown copper films was observed only at a thickness exceeding 200 nm .¹⁹ The sharp rise in resistivity at thickness below $\sim 50 \text{ nm}$, even though films are continuous (as revealed by SEM and STM), can be explained semiquantitatively as arising from (a) perhaps on increased concentration of contaminants during early stages of deposition and (b) grain boundary and surface scattering.³⁵ The lowest resistivity value in our study was $2.9 \mu\Omega\text{-cm}$ for 1300 \AA thick Cu film. This relatively high resistivity compared to bulk copper ($1.67 \mu\Omega\text{-cm}$) can be attributed to the incorporation of carbon and oxygen during film growth as observed in XPS analysis. Figure 9 shows the atomic concentration depth profile determined by XPS of a copper film deposited on SiO_2 at $285 \text{ }^\circ\text{C}$, under 50 Torr reactor pressure. Increasing sputter time corresponds to deeper layers in the film. The observed high carbon and oxygen concentration in the top layers of the copper film is due to atmospheric contamination in the form of hydrocarbons and oxides. Surface contamination appeared to be removed after

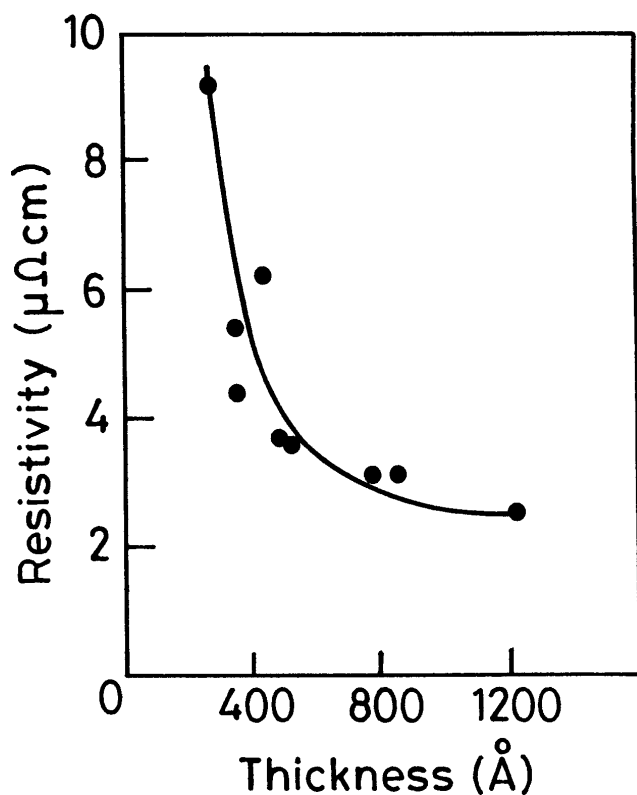


FIG. 8. Room temperature electrical resistivity of Cu films as a function of film thickness.

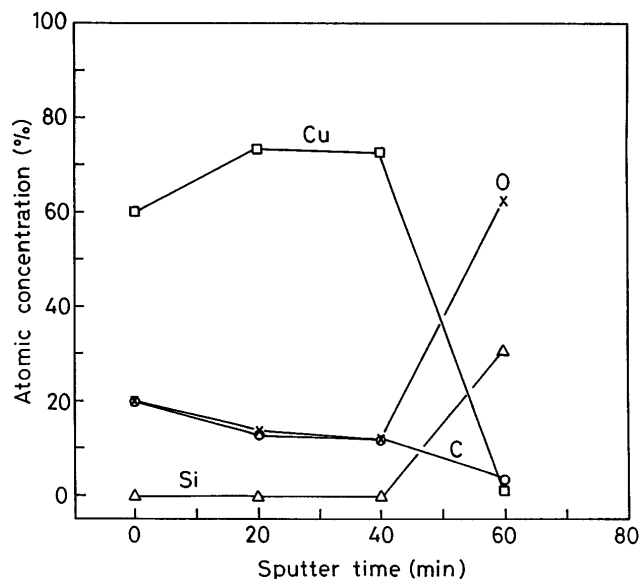


FIG. 9. Atomic concentration depth profile for Cu film as determined by XPS. Substrate temperature = $285 \text{ }^\circ\text{C}$, vaporizer temperature = $135 \text{ }^\circ\text{C}$, pressure = 50 Torr, and Ar carrier flow = 50 sccm.

20 min of sputtering. Atomic concentrations corresponding to the bulk of the copper film were then obtained. Results indicate the presence of 13 at.% carbon and 13.5 at.% oxygen. Simultaneous incorporation of carbon and oxygen in copper can be attributed to the decomposition of the organic ligand associated with the precursor due to pyrolysis in the chemically inert argon atmosphere. We have not observed any significant differences in resistivity of Cu films grown at different substrate temperatures ($225\text{--}350 \text{ }^\circ\text{C}$) and pressures ($10\text{--}50 \text{ Torr}$), for a similar film thickness. So, we believe that the carbon and oxygen contamination of the films is associated with the decomposition of $\text{Cu}(\text{tbaoc})_2$ in the argon ambient. Attempts are underway to study the deposition process using hydrogen as the carrier gas.

C. Mechanism of copper deposition

We propose a possible pyrolysis mechanism by which copper is produced from $\text{Cu}(\text{tbaoc})_2$. The pyrolysis of $\text{Cu}(\text{tbaoc})_2$ at a lower temperature than $\text{Cu}(\text{dpm})_2$ can be attributed to the presence of the *t*-butyl ester which triggers a decomposition pathway shown schematically in Fig. 10. In this mechanism, the *t*-butyl-acetoacetate anion (tbaoc) in the form of ester enolate can undergo a thermal "ene" type reaction³⁴ in a concerted pathway to produce isobutene and acetoacetate anion Y. Precedence exists in the literature for similar rearrangement (Ireland-Claisen) of ester enolates even under mild conditions ($25 \text{ }^\circ\text{C}$).³⁵ The next step involves the facile loss of CO_2 from Y and formation of acetone after hydrogen abstraction. The probable reason for the

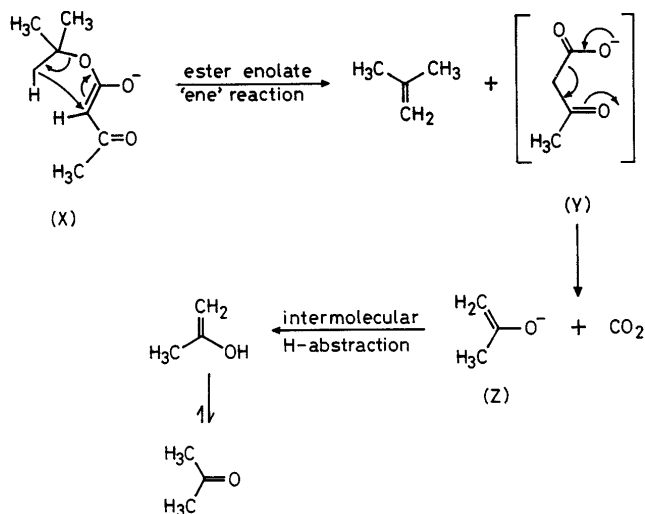


FIG. 10. Mechanism proposed for the decomposition of the ligand tbaoc.

low decomposition temperature of Cu(tbaoc)₂ is that (i) the Cu–O linkage from the ester moiety is weaker than the Cu–O linkage of the carbonyl group and (ii) the latter Cu–O bond cleaves easily as it yields the stable molecule acetone.

IV. CONCLUSIONS

A new, nonfluorinated β -diketonate complex, bis(*t*-butylacetoacetate)Cu(II), intended as a CVD precursor, was obtained by modifying Cu(dpm)₂. The complex is stable in air and does not decompose at low vaporizing temperatures. It has the advantage of having higher sublimation rate and lower decomposition temperature than Cu(dpm)₂. The lower decomposition temperature of Cu(tbaoc)₂ can be attributed to the thermal "ene" type reaction of the *t*-butylacetoacetate anion(tbaoc) in a concerted pathway to produce isobutene and acetoacetate anion and also to the facile loss of CO₂ resulting in the formation of acetone after hydrogen abstraction. Pyrolysis of Cu(tbaoc)₂ yielded mirror-bright copper films with highly dense and small grain structure, resulting in strong adherence of copper to SiO₂ substrate. Further, the well-connected nature of the grains at an early stage of growth led to resistivity of less than 4 $\mu\Omega$ -cm at thickness as low as 50 nm.

REFERENCES

1. *Chemical Vapor Deposition: Principles and Applications*, edited by M. L. Hitchman and K. F. Jensen (Academic Press, New York, 1993).
2. *Handbook of Chemical Vapor Deposition*, edited by H. O. Pierson (Noyes Publications, Park Ridge, NJ, 1992).
3. G. B. Stringfellow, *Organometallic Vapor Phase Epitaxy: Theory and Practice* (Academic Press, San Diego, CA, 1989).
4. *The Chemistry of Metal CVD*, edited by T. Kodas and Mark J. Hampden-Smith (VCH Publishers Inc., Weinheim, Germany, 1994).
5. *Thin Film Processes II*, edited by J. L. Vossen and W. Kern (Academic Press, Inc., Boston, 1991).
6. S. Oda, H. Zama, and S. Yamamoto, *J. Cryst. Growth* **145**, 232 (1994).
7. C. H. Warren, B. D. Seshu, and H. P. Cheng, *Chem. Mater.* **6**, 1955 (1994).
8. H. S. Park, M. Mokhtari, and H. W. Roesky, *Chem. Vap. Dep.* **2**, 135 (1996).
9. L. H. Dubois and B. R. Zegarski, *J. Electrochem. Soc.* **139**, 3295 (1992).
10. N. Awaya and Y. Arita, *Jpn. J. Appl. Phys.* **32**, 3915 (1993).
11. H. P. Chen and B. D. Seshu, *J. Am. Ceram. Soc.* **77**, 1799 (1994).
12. T. Kimura, H. Yamauchi, H. Machida, H. Kokubun, and M. Yamada, *Jpn. J. Appl. Phys.* **33**, 5119 (1994).
13. K-H. Dahmen and T. Gerfin, *Prog. Cryst. Growth and Charact.* **27**, 117 (1993).
14. V. A. C. Hannapel, H. D. van Corbach, T. Fransen, and P. J. Gellings, *Thin Solid Films* **230**, 138 (1993).
15. H-K. Shin, K-M. Chi, M. J. Hampden-Smith, T. T. Kodas, J. D. Farr, and M. Paffett, *Adv. Mater.* **3**, 246 (1991).
16. A. E. Kaloyeros and A. F. Michael, *MRS Bull.* **18**, 22 (1993).
17. S. P. Murarka and S. W. Hymes, *CRC Crit. Rev. Solid State Mater. Sci.* **20**, 87 (1995).
18. T. Ohmi and K. Tsubouchi, *Solid State Technol.* **35**, 47 (1992).
19. D. Kim, R. H. Wentorf, and W. N. Gill, *J. Electrochem. Soc.* **140**, 3273 (1993).
20. J. M. E. Harper, E. G. Colgan, C-K. Hu, J. P. Hummel, L. P. Buchwalter, and C. E. Uzoh, *MRS Bull.* **Aug.**, 23 (1994).
21. *The Chemistry of Metal CVD*, edited by T. T. Kodas and M. J. Hampden-Smith (VCH Publishers Inc., Weinheim, Germany, 1994), Chap. 4, p. 175.
22. Y. Pauleau and A. Y. Fasasi, *Chem. Mater.* **3**, 45 (1991).
23. D. Temple and A. Reisman, *J. Electrochem. Soc.* **136**, 3525 (1989).
24. M. J. Hampden-Smith and T. T. Kodas, *Polyhedron* **14**, 699 (1995).
25. S. K. Reynolds, C. J. Smart, and E. F. Baran, *Appl. Phys. Lett.* **59**, 2332 (1991).
26. T. H. Stumm and H. van den Bergh, *Mater. Sci. Eng.* **B23**, 48 (1994).
27. J. Goswami, Ph.D. Thesis, Indian Institute of Science, Bangalore (1995).
28. S. Patnaik, T. N. Guru Row, R. Lakshmi, Anjana Devi, J. Goswami, S. A. Shivashankar, S. Chandrasekaran, and W. T. Robinson, *Acta Crystallogr.* **C52**, 891 (1996).
29. K. J. Eisentraut and R. E. Sievers, *J. Inorg. Nucl. Chem.* **29**, 1931 (1967).
30. S. P. Murarka, R. J. Gutmann, A. E. Kaloyeros, and W. A. Lanford, *Thin Solid Films* **236**, 257 (1993).
31. S. P. Murarka and S. W. Hymes, *CRC Crit. Rev. Solid State Mater. Sci.* **20**, 87 (1995).
32. J. Li and J. W. Mayer, *MRS Bull.* **18**, 52 (1993).
33. Geetha Ramaswamy, A. K. Raychaudhuri, J. Goswami, and S. A. Shivashankar, *J. Phys. D.* (in press).
34. *Intramolecular Diels-Alder and Alder-Ene Reactions*, edited by D. Taber (Springer, New York, 1984), p. 61.
35. R. Ireland and M. Willand, *J. Am. Chem. Soc.* **98**, 2868 (1976).